Zoological Studies **61**:80 (2022)
doi:10.6620/ZS.2022.61-80

Zoological Studies

Open Access

The Dung Beetle *Oxyomus* of Taiwan (Coleoptera: Scarabaeidae): Review of the Fauna, a New Species and its Larva Associated by DNA Barcoding

Bin-Hong Ho[1], Fang-Shuo Hu[1], and Martin Fikáček[1,2,*]

[1]*Department of Biological Sciences, National Sun Yat-sen University, Kaohsiung 804, Taiwan. *Correspondence: E-mail: mfikacek@gmail.com (Fikáček). E-mail: binhongho0505@smail.nchu.edu.tw (Ho); fangshuo_hu@smail.nchu.edu.tw (Hu)*
[2]*Department of Entomology, National Museum, Cirkusová 1740, Praha 9, Czech Republic*

Received 22 May 2022 / Accepted 7 October 2022 / Published 22 December 2022
Communicated by Shen-Horn Yen

The Taiwanese fauna of the dung beetle genus *Oxyomus* Dejean, 1833 (Coleoptera: Scarabaeidae: Aphodiinae) is reviewed based on museum specimens and newly collected material. Four species, all endemic to Taiwan, are recognized, one of which is newly described here: *O. alligator* sp. nov. Remaining species are diagnosed, compared with similar relatives from outside of Taiwan, and their distribution is mapped. We show that Taiwanese *Oxyomus* species form three distinct morphological groups, similar to species from Japan, SE Asia and Malay Archipelago, respectively, indicating a possible composite origin of Taiwanese fauna. The species occur in submontane and montane forests at altitudes of 700–2550 m including the secondary *Cryptomeria* ones. Available data confirm their association with dung of various forest mammals (monkeys, muntjacs and serows), although the discovery of larvae in sifted forest leaf litter may indicate they can also develop in nutrient-rich substrate around the dung. The larva of *O. alligator* sp. nov. is described in detail, based on the larval specimens associated with adults by DNA barcodes. Larvae of *Oxyomus alligator* sp. nov. are similar to those of the European *O. sylvestris* (Scopoli, 1763), with important differences only found on maxilla and abdominal apex.

Key words: Aphodiinae, Dung beetles, *Oxyomus*, Taiwan, New species, Immature stages, DNA barcoding, Distribution, Endemism.

BACKGROUND

The forest canopy was long considered to host the most diverse arthropod and beetle communities (*e.g.*, Erwin 1982), but, surprisingly, the forest soil and leaf litter was found to be just as diverse as the canopy (Nadkarni and Longino 1990; Stork and Grimbacher 2006). Although the forest floor is easier to access than tree canopies, our knowledge of its fauna remains very poor. For most groups, the data indicating high species diversity are expert estimates based on museum collections or DNA-based analyses of bulk samples (metabarcoding: Andújar et al. 2015; Arribas et al. 2020); information about systematics, biology or immature stages is absent. Integrative systematics combining morphology and DNA-based approaches have recently proven to be promising for better understanding the leaf litter arthropods and beetles (*e.g.*, Huang and Lin 2010; Tsai and Yeh 2016). Our recently started survey of Taiwanese leaf litter beetles adopted this approach, and immediately led to the discovery of previously unknown beetle species, their immature stages, and basic information about their biology.

Several genera of scarab beetles (Scarabaeidae) have been occasionaly collected from forest leaf litter (*e.g.*, *Sinodrepanus* Simonis, 1985, *Onthophagus*

Citation: Ho BH, Hu FS, Fikáček M. 2022. The dung beetle *Oxyomus* of Taiwan (Coleoptera: Scarabaeidae): review of the fauna, a new species and its larva associated by DNA barcoding. Zool Stud **61**:80. doi:10.6620/ZS.2022.61-80.

Latreille, 1802, *Liatongus* Reitter, 1892, *Panelus* Lewis, 1895 and *Haroldius* Boucomont, 1914) (Paulian and Scheuern 1994; Ochi 2012), despite being primarily associated with mammal dung. Several aphodiine groups inhabit other decaying organic substrates than dung, such as rotten wood and moss (*e.g.*, *Saprosites* Redtenbacher, 1858) (Stebnicka 2013) or roots and litter of seashore or riverside habitats (*e.g.*, *Odochilus* Harold, 1877, *Psammodius* Fallen, 1807, *Rakovicius* Pittino, 2006 and *Trichiorhyssemus* Clouët, 1901) (Pittino and Kawai 2007; Ochi et al. 2011; Ho 2021). The genus *Oxyomus* Dejean, 1833, with ca. 25 described species occurring in the Oriental, Palaearctic and southern Nearctic regions. Three species of *Oxyomus* have been described from Taiwan, all of them endemic to the island (Nomura 1973; Masumoto et al. 2014 2018). *Oxyomus* species are occasionally found on the dung of forest mammals (*e.g.*, sambars or monkeys), but more frequently have been sifted from forest leaf litter; their biology remains unknown (Dellacasa and Stebnicka 2001; Masumoto et al. 2014; Schoolmeesters 2022).

Our sampling of leaf litter in central Taiwan resulted in a discovery of dung-beetle larvae which we succeeded to associate with co-occurring *Oxyomus* adults by DNA barcoding. Besides helping to understand the biology of *Oxyomus*, larval morphology also provides valuable data for the phylogenetic reconstruction and higher classification (*e.g.*, Ahrens 2006; Grebennikov and Scholtz 2004; Philips 2016; Šípek et al. 2009). Still, larval morphology is poorly known for most Aphodiinae. Despite being diverse in the Oriental region, only the larva of a single aphodiine species, *Colobopterus quadratus* (Reiche, 1847), has been described (Li et al. 2019). Within *Oxyomus*, larva is only known for the European *O. sylvestris* (Scopoli, 1763) (Jerath 1958 1960). In this study, we review the Taiwanese species of the leaf-litter inhabiting dung beetle genus *Oxyomus*, describe the new species discovered during our survey and its larva, and summarize the data about the biology derived from examined specimens. It is the first of the prepared studies aiming at better understanding the diversity of leaf litter beetles in Taiwan and their ecological importance in tropical forests.

MATERIALS AND METHODS

Material collecting and depository

DNA work

The complete genomic DNA was extracted from adults (n = 4) of *Oxyomus alligator* sp. nov. and its putative larvae (n = 2), using the Tissue Genomic DNA Mini Kit (Geneaid Biotech Ltd, New Taipei, Taiwan) following the manufacturer's protocol (lysis temperature = 60°C), but with adapted incubation periods (14 hours in proteinase K + GT buffer, 1 hour in proteinase K + GT buffer + LGT buffer). We amplified the 5′ fragment of the cytochrome oxidase I (*CO1*) mitochondrial gene using the standard LCO1490/HCO2198 primers (Folmer et al. 1994) with the following PCR protocol: 94°C for 3 min, 35 × (94°C for 0:30 min, 48°C for 0:45 min, 72°C for 1:00 min), 72°C for 8 min. Sequences were checked for potential sequencing errors, manually edited, and aligned with sequences of *Oxyomus sylvestris* (Scopoli, 1763) and *Aphodius fimetarius* (Linnaeus, 1758) downloaded from Barcoding of Life Database (BOLD) using the MUSCLE algorithm in Geneious ver. 6.1. Analyses of the final aligned dataset were performed in MEGA 7.0 (Kumar et al. 2016): mean genetic distances between and within each species were calculated using uncorrected p-distances, and a maximum likelihood species tree was built, implementing the most general GTR model with rate heterogeneity along the sequences (+G) and the presence of invariant sites (+I). Bootstrap supports were calculated based on 100 replicates. Newly generated *CO1* sequences of *O. alligator* sp. nov. were submitted to BOLD under sequence numbers TWOXY001-22 to TWOXY006-22. All vouchers were collected in Taiwan, Nantou County, Huisun Forest Reserve (see material examined for details). GenBank numbers for sequences downloaded from BOLD Systems are provided in figure 1.

Examined specimens were deposited into the following collections: NMNS, National Museum of Natural Science, Taichung, Taiwan (Jing-Fu Tsai); NMPC, National Museum, Prague, Czech Republic (L. Sekerka, J. Hájek); NCHU, Department of Entomology, National Chung Hsing University, Taichung, Taiwan (Man-Miao Yang); TARI, Taiwan Agriculture Research Institute, Taichung, Taiwan (Chi-Feng Lee); BHHC, Bin-Hong Ho private collection, Taipei, Taiwan; CCLI, Chun-Lin Li private collection, Nantou, Taiwan.

Adult morphology and systematics

Adults were dry-mounted on white cardboard label, and the dissected epipharynx was embedded into a drop of alcohol-soluble Euparal resin on small pieces of cover glass attached under the specimen. All specimens were examined by Olympus SZ51 stereomicroscope. Photographs of adults and of the aedeagus were taken using an Olympus O-MD em-5 mark II digital camera with Laowa 25 mm f2.8 2.5-5x ultra macro lens. The photographs of the epipharynx were taken taken by

Canon EOS 650D digital camera attached to a Zeiss Axioskop 2 microscope. All photographs were stacked in Helicon Focus 8 software. Measurements were taken using a Leica M205 C stereomicroscope and a Leica MC170 HD digital camera with LAS software (version 4.4.0, Leica Application Suite, Wetzlar, Germany) or digital caliper. All measurements are given in millimeters and abbreviated as follows: BL: body length from the anterior margin of the clypeus to the elytral apex; HL: head length between anterior margin of clypeus and anterior margin of the pronotum; HW: maximum width of the head; PL: pronotum length from anterior margin to the posterior margin of the pronotum; PW: maximum width of the pronotum.; EL: length of elytron between humeral tooth and elytral apex.; EW: maximum width of elytra. For the collection data, separate to different labels are used double slashes (//), and the supplementary data are provided in square brackets [ ]. GPS coordinates are cited as listed on the labels. The distribution map was constructed in R and subsequently adapted in InkScape. The terminology of epipharynx follows Dellacasa et al. (2010).

Larval morphology

We examined four field-collected larvae, representing the second and third larval instars. Two larvae (one per each instar) were used for DNA barcoding. These larvae were properly cleaned of muscles during the DNA extraction using proteinase K. Additional larvae were photographed and then cleaned in 10% KOH solution overnight. All larvae were examined in temporary glycerine slides without any additional treatment; mouthparts were partially dissected. Morphological terminology follows Verdu and Galante (2000). Habitus photographs were taken using a Canon EOS 550D digital camera with attached Canon MP-E65 mm f/2.8 1–5× macro lens and stacked in Helicon Focus software. Slide-mounted larvae were examined using Leica CME compound microscope; working photographs were taken using the camera attached to the microscope using the AmScope CA-CAN-SLR adapter. Drawings of larval morphology were traced from the working photographs in the Clip Studio Paint software using the Wacom graphic tablet. After the publication of this study, the larvae will be re-mounted on the permanent Euparal slides and deposited into the collection of NMNS. All working photographs used in this study were uploaded to the Zenodo archive under doi:10.5281/zenodo.7124078.

RESULTS

DNA barcoding

The sequenced specimens of *Oxyomus alligator* sp. nov. (6 specimens, all from Huisun Forest reserve) provided highly similar *cox1* sequences (*p*-distance 0.3–1.5%, mean 1.0%), confirming the species identity of the larvae described below (Fig. 1). The available barcodes of *O. sylvestris* from Germany and Finland (17 specimens) show a more uniform genetic structure of this species across Europe (*p*-distance 0.0–0.6%, mean 0.25%). *Oxyomus alligator* sp. nov. shows a similar genetic distance from *O. sylvestris* (mean *p*-distance 15.8%) and from *Aphodius fimetarius* used as an outgroup (mean *p*-distance 18.2%).

Key to Taiwanese *Oxyomus* species

1. Each elytron with 8 visible costae (sutural one counted, marginal one not, Fig. 2C). Pronotum with the longitudinal median groove (Figs. 2A, 2G, 7D) .... *O. alligator* sp. nov.
- Each elytron with 10 visible costae (sutural one counted, marginal one not, Fig. 7J, 7K). Pronotum without longitudinal median groove (Fig. 7A–C) 2
2. The first elytra interval with two well-separated rows of punctures thorought; both rows clearly separated at the level of metathorax, parameres longer and apex rather slender (Fig. 7I, 7G) .... *O. taipingensis* Masumoto, Kiuchi & Wang, 2014
- The first elytra interval with two rows of punctures gradually fused towards apex; only a single row is present at the level of metathorax, parameres shorter and apex moderately rounded (Fig. 7E–F, 7H) 3
3. Punctures on pronotal disc with very short setae, setae not reaching neighboring punctures (Fig. 7O). Elytral costae without micro-setae (Fig. 7M). 5th elytral costa long and strongly developed, reaching as far as 7th costa (Fig. 7K) .... *O. nanxiensis* Masumoto, Kiuchi & Wang, 2018
- Punctures on pronotal disc with longer setae, setae reaching neighboring punctures (Fig. 7N). Elytral costae with micro-setae (Fig. 7L). 5th costa short and low, not reaching as far as 7th costa (Fig. 7J) .... *O. masumotoi* Nomura, 1973

Oxyomus alligator sp. nov.

(Figs. 2, 3A–B, 4–6, 7D)
urn:lsid:zoobank.org:act:4459987B-3F18-480A-A133-07D7F952E3CE

Type material: HOLOTYPE in NMNS: ♂, TAIWAN: Nantou county, Huisun Forest reserve, track to Xiaochushan Mt., 24.0847025°N, 121.0274161°E, 1000 m, 4.V.2019; Damaška, Fikáček, Hu & Liu lgt., 2019-TW16// Huisun Leaf Litter Beetles Project, Additional specimen: HS3-015. PARATYPES in NMNS, TARI, NCHU, NMPC, BHHC, CCLI: TAIWAN: Taichung City: 1♂ 3♀, Heping Township, Wushikeng, alt. 1050 m, 24°16'23.3"N 120°56'59.6"E, leaf litter, 28.VII.2019, W.Z. Tseng leg.// BHPC 000-

0894; BHPC 000-0895; BHPC 000-0896; BHPC 000-0897. 1♂, Heping Township, Dasyueshan logging rd. 31.5 km, 24.22700°N, 120.97283°E, alt. 2020 m, 1.V.2018, B.H. Ho leg.// BHPC 000-0891. Nantou County: 4exs, same data for the holotype. 1♀, Huisun Forest reserve, track to Xiaochushan Mt., 24.0847025°N, 121.0274161°E, 1000 m, 4.V.2019; Damaška, Fikáček, Hu & Liu lgt., 2019-TW16// mixed conifer/broadleaf forest + sparse broadleaf forest on the slope: sifting// Huisun Leaf Litter Beetles Project, DNA extraction: HS3-015. 1ex, Huisun Forest reserve, track to Xiaochushan Mt., 24.0744602°N, 121.0366337°E; 1150 m, 4.V.2019; Damaška, Fikáček, Hu & Liu lgt., 2019-TW14// primary forest on the slope with sparse understory: sifting of small accumulations of leaves// Huisun Leaf Litter Beetles Project, DNA extraction: HS1-009. 1ex, Huisun Forest reserve, track to Xiaochushan Mt., 24.0744602°N, 121.0366337°E; 1150 m, 4.V.2019; Damaška, Fikáček, Hu & Liu lgt., 2019-TW14// primary forest on the slope with sparse understory: sifting of small accumulations of leaves// Huisun Leaf Litter Beetles Project, Additional specimen: HS1-009. 2♀, Ren-ai Township, Huisun forest area, by FIT, 28.III-5.V.2019, F.S. Hu & W.R. Liang leg. 1♂, Ren-ai Township, Huisun forest area, by FIT, 1-13.IV.2018, B.H. Ho & W.R. Liang leg.// BHPC 000-0510. 1ex, Huisun Forest reserve, track to Xiaochushan Mt., 24.0744602°N, 121.0366337°E; 1150 m, 24.ii.2020; F.-S. Hu, 20-02HS5// primary forest on the slope with sparse understory: sifting of accumulations of leaves// DNA voucher specimen 20-02HS504. 1ex, Huisun Forest reserve, track to Xiaochushan Mt., 24.0847025°N, 121.0274161°E, 1000 m, 24.ii.2020; F.-S. Hu, 20-02HS3// mixed conifer/broadleaf forest + sparse broadleaf forest on the slope: sifting// DNA voucher specimen 20-02HS304. 1ex, Huisun Forest reserve, track to Xiaochushan Mt., 24.0847025°N, 121.0274161°E, 1000 m, 15.i.2022; Fikáček & Yu lgt., 22-02-HS3// mixed conifer/broadleaf forest + sparse broadleaf forest on the slope: sifting; many *Dolichoderus* ants// 22-01HS304. 5ex, Huisun Forest res.,Wading trail, 24.0892139°N, 121.0297836°E, 700m; 17.viii.2021; Fikáček & Liang lgt., 21-08HS5// Stony forest on the slope, small leaf accumulations// 21-08HS502. 2ex, Xinyi, near Caopingtou, alt. 1200 m, 23.561188°N, 120.882372°E, 12.IV-22.V.2018, I.C. Wang & S.P. Kao leg. (FIT). Kaohsiung City: 1ex, Maolin Dist., Duona Logging Road 9.3 km, by FIT, 16.II-16.III.2019, C.T. Hsu leg. Pingtung County: 1ex, Taiwu, Mt. Kavulungan Trailhead, 22.61479°N, 120.69983°E, alt. 1250 m, 30.VII.2022, F.S. Hu leg. (leaf litter). 1 ex, Mt. Ritangzhen trail, lower part, 1450 m,

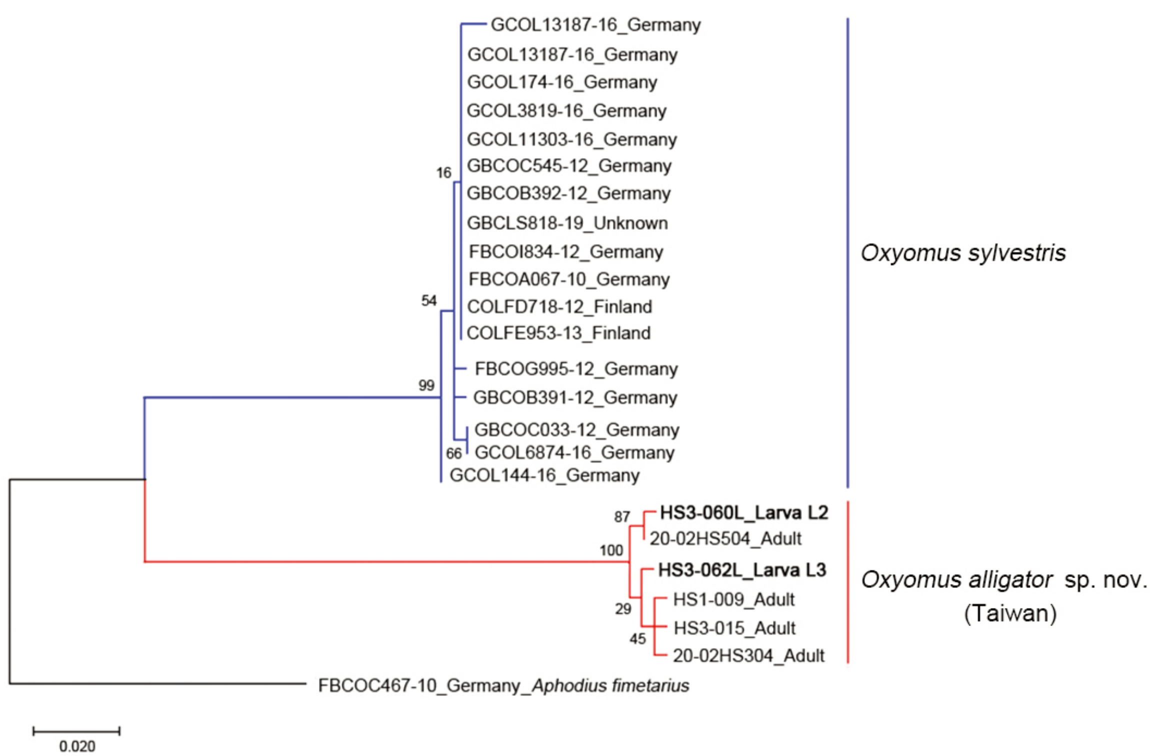

Fig. 1. Maximum likelihood analysis of available *cox1* sequences of *Oxyomus*, with *Aphodius fimetarius* as an outgroup. Accession numbers and country of origin are provided for sequences from BOLD. Sequenced larvae of *O. alligator* sp. nov. used for the morphological description are highlighted.

22.622302, 120.703677, 10.ix.2022, Fikáček, Ho, Peng lgt. TW2022-009// submontane broadleaf forest with intermixed conifers (Cupressaceae) and moderately dense understory, small to large accumulation of leaves.

Larval material examined: 2 L2 larvae (vouchers HS3-060L, one larva sequenced); 2 L3 larvae: (vouchers HS3-062L, one larva sequenced): TAIWAN: Nantou county: Huisun Forest reserve, track to Xiaochushan Mt., 24.0847025°N, 121.0274161°E, 1000 m, 4.v.2019, Damaška, Fikáček, Hu & Liu lgt. All specimens

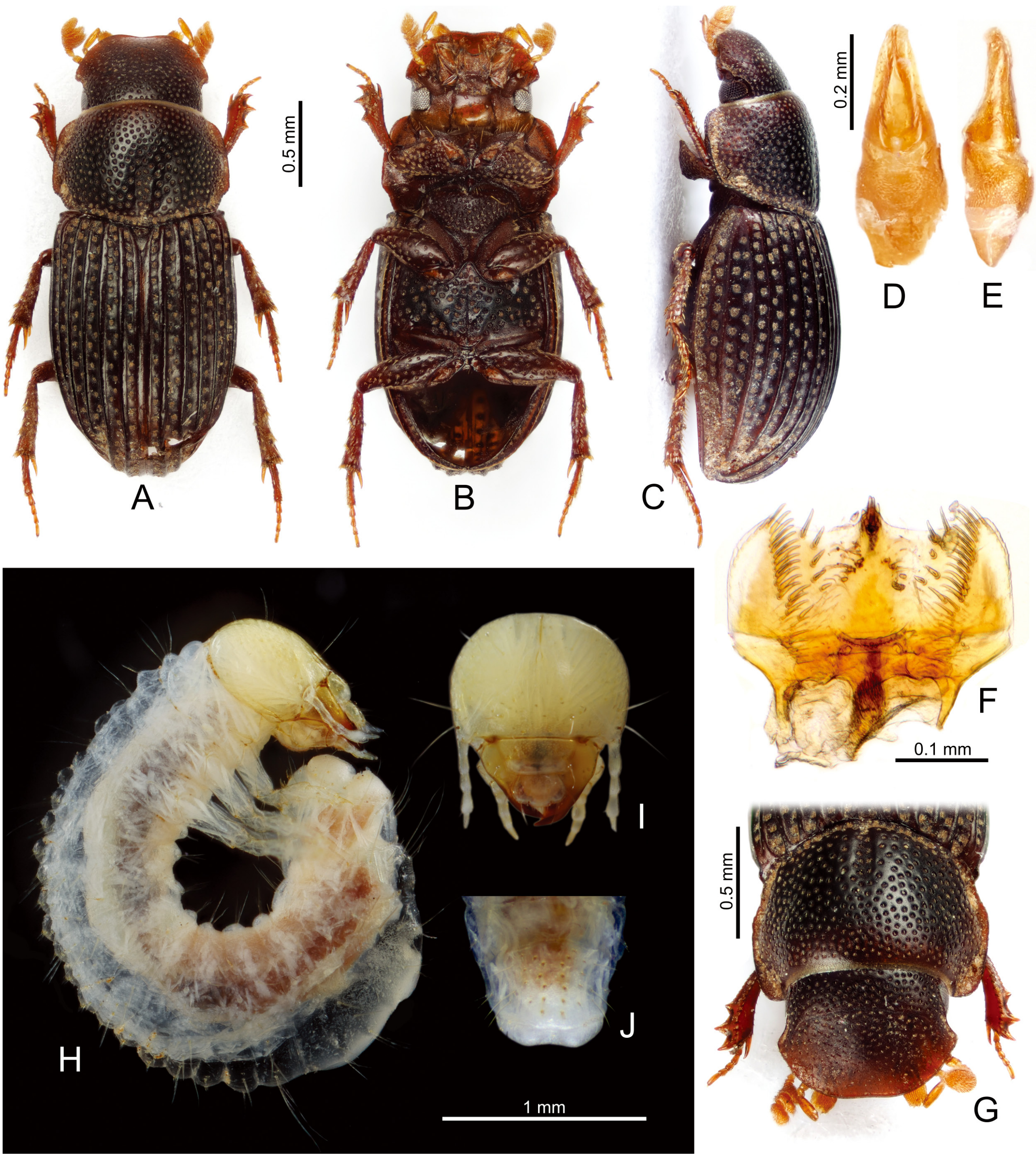

Fig. 2. *Oxyomus alligator* sp. nov.: adult (A–G) and larva (H–J). A–G, male holotype (A, dorsal view; B, ventral view; C, lateral view; D–E, aedeagus; F, epipharynx; G, detail of head and pronotum). H–J, third instar larva, additional non-sequenced specimen HS3062L (H, lateral view; I, head in dorsal view; J, ventral surface of the abdominal apex).

deposited in NMNS.

Description of holotype: Male, body length 2.48 mm. Body oblong-ovate, surface mostly brownish black mixed with reddish brown, rather strongly convex posterior-dorsal, weakly shiny or rather dull.

Head: Moderately convex in posterio-median portion, surface microreticulate, clypeus with scattered slightly transverse punctures; with rounded punctures on frons; each puncture with an extremely short yellowish seta. Clypeus dark reddish brown, coarsely, with punctures at sides coarser than mesally; anterior margin of clypeus indistinctly emarginate mesally, widely rounded at sides, with continuous narrow border. Eyes present, inserted into head, rounded, weakly convex laterally in dorsal views, distance between eyes about 12 times the eye transverse diameter. Antennae yellowish brown, with 9 antennomeres.

Pronotum: Surface microreticulate, moderately shining, convex, coarsely and densely punctate, punctures rounded, separated by ca. their diameter, each puncture with an extremely short yellowish seta. Posterior portion with a transverse row of coarse punctures along posterior margin; posteromesal portion with deeply impressed longitudinal groove; anterior and posterior margins strongly bordered. Pronotal anterior angles well-defined in dorsal view, dark reddish-brown, rounded, with well-developed border at sides; posterior angles strongly oblique, weakly emarginate. Posterior margin deep, beaded.

Scutellar shield: Small, elongate triangular, surface micro-reticulate and dull, with very weak median carina, punctures rounded, concentrated laterally near anterior margin.

Elytra: Sub-ovate, basal portion truncate, 1.5 times as long as wide, widest at midlength, 1.9 times the length and 1.1 times the width of pronotum; moderately convex in lateral view, highest at basal 3/4. Disc with 10 costae and 10 intervals (marginal groove not counted); costae narrow, with micro-reticulate weakly shining surface, not combined before apex. 8^{th} and 10^{th} costae invisible, 2^{nd} to 5^{th} and 7^{th} costae becoming stronger than others, 1^{st}, 6^{th} and 9^{th} costae weaker than others. 1^{st} to 3^{rd} and 7^{th} costae the longest, 6^{th} costa the shortest; 4^{th} costa shorter than 5^{th} costa, reaching as far posteriorly as 9^{th} costa. 6^{th}, 7^{th} and 9^{th} costae connected at humeral area. Intervals deeply concave, opaque and dull. 1^{st} and 6^{th} to 10^{th} intervals each with single row of punctures, 7^{th}+8^{th} intervals and 9^{th}+10^{th} intervals combined, seemingly very wide and with two rows of punctures; 2^{nd} to 5^{th} intervals with two rows of staggered punctures. All punctures rather large, round to slightly ovate. Humeral tooth acute, short and strong, obtusate at apex, forming nearly right angle.

Ventral side: Prosternum coriaceous and micro-reticulate, raised in anteromedial part, concave at sides. Mesoventrite microsculptured, with concentrated, subovate or rounded punctures. Metaventrite weakly convex, with flat mesal part, bearing a longitudinal, extremely narrow and deep median groove with irregularly scattered shiny, subovate or rounded punctures. Each puncture with an extremely short, small, yellowish seta. Abdomen coriaceous, micro-reticulate, with rounded apex.

Legs: Reddish brown, shiny; femora stout, surface weakly microsculptured in ventral view, surface of profemora with closely ovate punctures; surface of meso- and metafemora with moderately-sized scattered ovate punctures, each puncture with an elongate yellowish seta. Protibiae with three strong external teeth, proximal portion serrate at outer margin, with an acute terminal spur, gently curved in ventral view. Meso- and metatibiae moderately widened apically, with two weakly transverse carinae, apically with fimbriate spinules, short, of unequal length. Mesotibiae with two terminal spurs, the upper one about 2/3 times in length of the 1^{st} mesotarsomere, the lower one ca. half the length of the upper one. Metatibiae with two terminal spurs, the longer one ca. 3/5 times the length of the 1^{st} metatarsomere, shorter one ca. half the length of the 1^{st} metatarsomere. Claws small, regularly curved, slender.

Aedeagus (Fig. 2D–E): Basal piece widest in middle, strongly convex, slightly depressed behind anterior margin. Parameres simple, tapered in apical half, apex rounded, slightly bent ventrally in lateral view.

Epipharynx (Fig. 2F): Transverse, nearly rectangular, lateral sides nearly straight, front angles slightly curved. Corypha with 5 longitudinal celtes: two celtes very long in middle, additional three celtes very short at sides; celtes on tylus extremely short, not obvious. Chaetopedia with 5 celtes on each side, 1^{st} to 5^{th} gradually shorter. Chaetopariae long with densely, at least have 16 developed celtes on each side. Prophobae and apophobae scattered, not obvious. Mesophoba long, densely, rather macrosetation, inclined to left side. Dexiotorma and laetorma longitudinal, simple, rather slender in apex, almost equal in length.

Female: Lateral margin on pronotum less widened anteriorly, elytral 6^{th} costa usually longer than in male.

Measurements (in mm, n = 27, holotype + range for all specimens measured): BL: 2.48 (2.48–3.18); HL: 0.36 (0.32–0.41); HW: 0.75 (0.75–0.91); PL: 0.70 (0.70–0.94); PW: 1.00 (1.00–1.24); EL: 1.44 (1.44–1.93); EW: 1.07 (1.07–1.39).

Diagnosis of adult: *Oxyomus alligator* sp. nov. resembles *O. kocoti* Minkina, 2018 from northern Thailand (Chiang Mai: Doi Anghhang, Fig. 3C–D), by a similar shape of pronotum and elytral costae. It can be distinguished from *O. kocoti* as follows: (1) pronotum with longitudinal median groove; (2) pronotum more strongly convex in lateral view; (3) pronotum with well-developed lateral margin; (4) elytral 8th costa invisible; (5) elytral costae strongly developed and moderately shiny; (6) each puncture with an extremely short, yellowish seta. In Taiwan, *O. alligator* sp. nov. can be distinguished from other species of *Oxyomus* by the pronotum with a developed longitudinal median groove, well-developed lateral margin of the pronotum, and strongly developed elytral costae.

Etymology: The specific name, *alligator*, refers to the resemblance of the elytral surface of this species to the alligator skin.

Distribution: *Oxyomus alligator* sp. nov. is only known from Taiwan. It is widespread in the mountain areas of central and southern Taiwan where it occurs in altitudes between 700–2020 m. At the moment, it is recorded from the following regions: Taichung City, Nantou County, Kaohsiung City and Pingtung County. (Fig. 8).

Biology: *Oxyomus alligator* sp. nov. inhabits the dung masses of muntjac *Muntiacus reevesi* (Ogilby) and Formosan serow *Capricornis swinhoei* (Gray) in broad-leaved forest, mixed forest or secondary *Cryptomeria*. In Dasyueshan will sympatric with *O. taipingensis* Masumoto, Kiuchi & Wang.

Larval morphology (third instar larva) (Figs. 2H–J, 4E–F, 5A–D, 5H–K, 5M–R, 6A, 7A–F, 7M–N): *Body*: C-shaped, arched at abdominal segment 5. Head capsule yellowish brown; thoracic and abdominal segments membranous, whitish in color. Head appendages and legs very pale yellow; mandibles brown to dark brown on apex. Length of the body in uncoiled position (including head): 4.2 mm; maximum width of thorax: 0.8 mm.

Head (Fig. 4C): slightly wider than high (width: 0.81 mm; length: 0.80 mm, height: 0.43 mm). Head capsule with 6 longer setae (two along anterior margin, two anterolaterally, two dorsally) and two short setae (one anteromesally, one posteromesally) plus numerous minute setae and pore-like sensilla on whole surface. Epicranial sulcus present, frontal sulci not developed. *Clypeus* transverse, each half with a long lateral setae, one pore-like sensillum and one short setae situation slightly more mesally, and a small group of minute pores and microsetae at lateral margin. *Labrum* weakly trilobed and anterior margin; dorsal surface with a pair of long setae submesally and a short seta and a pore-like sensillum situated posteriorly of each long seta; lateral margin on each side with a long seta at midlength, and a short seta anteriorly and posteriorly of the long one. Epipharynx (Fig. 4F) with rather indistinct clitrae, anterior margin with moderately long setae laterally and mesally, and with a pair of long stout setae sublaterally. Protophoba ca. as wide as long, consisting of rather short but wide cuticular projections. Epitorna narrow, slightly asymmetric. Pternotormae asymmetric, the right

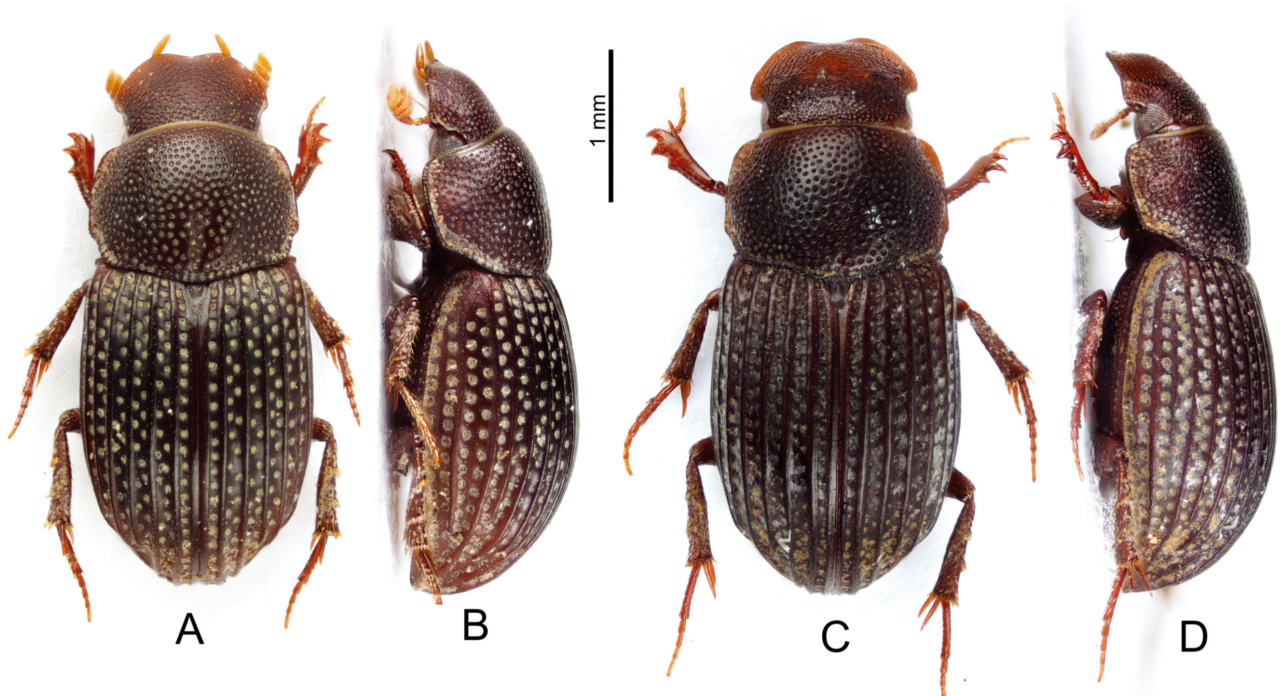

Fig. 3. The comparison of the females of *Oxyomus alligator* sp. nov. (A–B, paratype) and *O. kocoti* Minkina, 2018 (C–D, holotype).

one more robust than the left one.

Antenna (Fig. 5H–I): four-segmented, the basalmost segment with two weakly delimited pseudosegments. Antennomere 1 ca. as long as antennomere 3, antennomere 2 ca. as long as antennomere 4, half the length of antennomere 1. First antennomere without sensilla. Second antennomere with five small basal pores, two dorsally

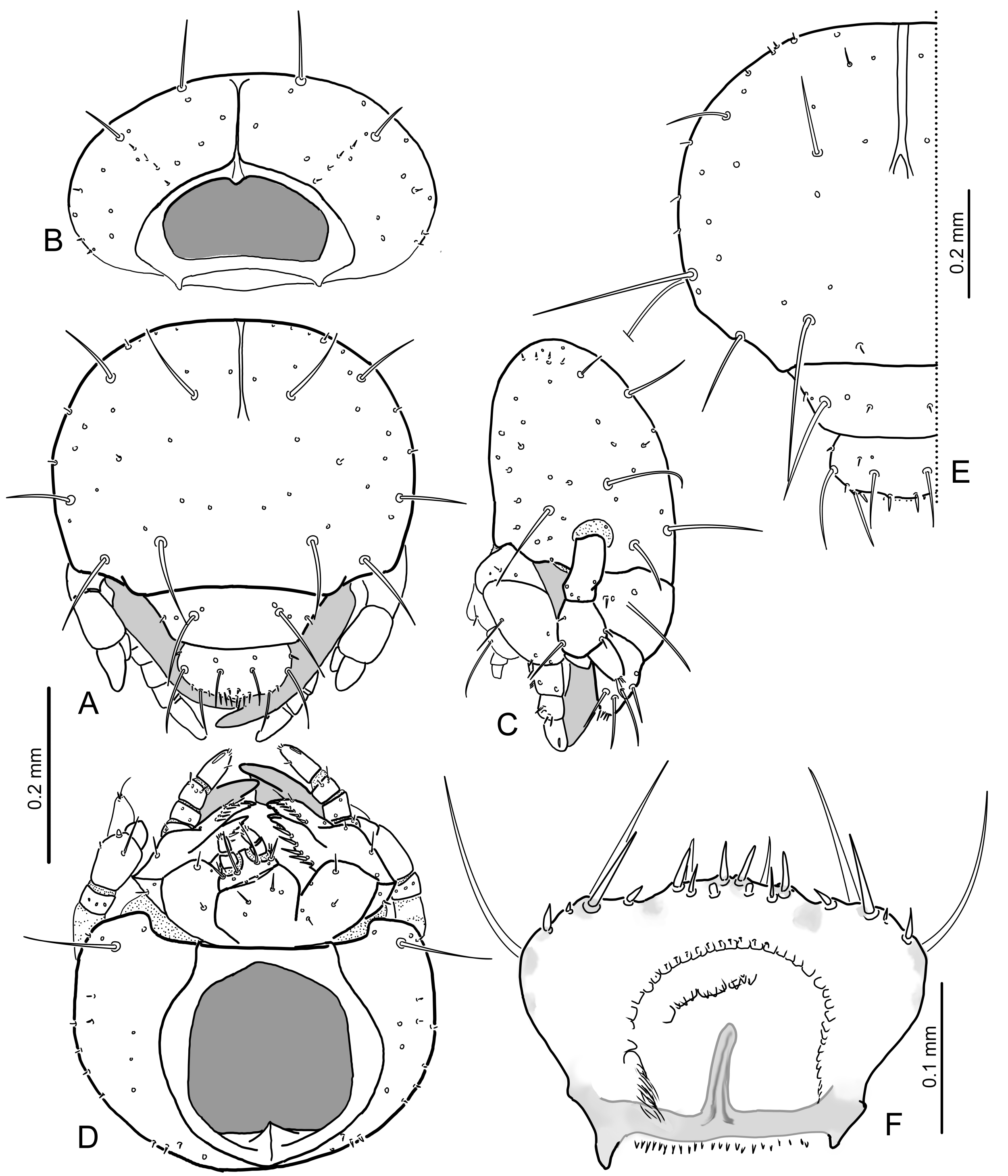

Fig. 4. Head morphology of the larva of *Oxyomus alligator* sp. nov. A–D, head of the second instar larva, sequenced specimen HS3_060L (A, dorsal view; B, posterior view; C, lateral view; D, ventral view). E, chaetotaxy of the dorsal surface of the head capsule of the third instar larva (HS03_62L, sequenced specimen). F, epipharynx of the third instar larva (HS03_62L, sequenced specimen).

on the segment, three ventrally on the intersegmental membrane. Third antennomere with six setae in a distal portion, two moderately long and one short dorsally, three moderately long dorsally. Sensorium situated dorsomesally, massive, wider and ca. half as long as fourth antennomere. Fourth antennomere conical, narrowing apically, inner sensorial field large, extending to ventral and dorsal surfaces, larger in dorsal view; apex with numerous microsetae and one long hair-like seta.

Mandibles (Fig. 5M–R): massive, strongly sclerotized especially on apex and in mola, slightly asymmetrical; each mandible with three pore-like sensilla, two short setae and one moderately long seta on dorsolateral surface; both mandibles with a small basal projection on ventral surface. Right mandible with tridentate apex, the middle tooth widely spatulate; mola elongate, constricted in the middle; distal base of mola with a short seta and a small group of short cuticular setae. Left mandible with bidentate apex, both teeth narrow; mola rounded in mesal view, its base with a bunch of long hair-like cuticular projections.

Maxilla (Fig. 5A–D): Cardo small, subtriangular, with one pore and two short setae; mesal submembranous area with two setae. Stipes slightly shorter than cardo; lacinia longer but situated more basally, left one with tridentate apex, right one bidentate apically; galea shorter but situated more distally, with unidentate apex on both sides. Chaetotaxy and surface structures asymmetrical on stipes, lacinia and galea: Both left and right stipes dorsally with two pores and two setae, and with one short setae ventrally on palpiger; ventral surface of stipes with two stout setae and a moderately large cuticular projection distally; basal pars stridens with 6 teeth in left stipes, and four teeth in right stipes. Left lacinia ventrally with a series of 6 stout setae directed ventromesad, and a long stout subapical seta directed mesad, and a fine long trichoid seta apically; dorsal surface with a subbasal moderately stout seta. Right lacinia ventrally with a series of 6 very long and stout setae and an apical trichoid seta; dorsal surface with moderately long subbasal setae and one stout and one short subapical setae. Left galea apically with two setae, one long and sickle-shaped, one trichoid, ventral surface with a series of large irregularly shaped cuticular projections and two pores subbasally, and with a mesal comb of plate-like cuticular projections mesally. Right galea with the same two apical setae, but ventrally with a series of three stout long setae, dorsally with a series of 8 moderately long trichoid setae. Maxillary palpus with four palpomeres, of the same shape and chaetotaxy in left and right maxilla; palpomere I shortest, with one short and two pore-like sensilla; palpomere II with two pore-like sensilla; palpomere III with two pore-like sensilla and two short setae situated near distal margin; palpomere IV the longest, with a dorsal digitiform sensilla and a ventral short setae, and a small apical sensorial area.

Labium (Fig. 5J–K): Mentum transverse, with a pair of short setae and a pair of pore-like sensilla near distal margin. Prementum slightly transverse, with a series of long to moderately long setae along articulation of each labial palpus, two pores on ventral surface and a pair of short setae and two pairs of pores between palpal articulations; ligula absent. Labial palpus short, with two palpomeres, with a small pore on intersegmental membrane between palpomere I and II. Hypopharynx with massive strongly asymmetrical oncyli, and slightly asymetrical arcs of cuticular hairs and setae on each side; the right one continuous, with basal portion with short cuticular hairs and anterior series of setae become spatulate towards an anterior apex; the left one discontinuous, with basal portion of hair-like cuticular projections and few moderately large basal teeth, and anterior part with a series of trichoid setae; anterior margin of hypopharynx with a transverse series of minute tooth-like cuticular projections.

Thorax (Fig. 6A): Prothorax on each side with 10 setae of variable lengths, meso- and metathorax each with 7 setae of variable length on each side, situated in an irregular row. Thoracic spiracle large, cribrate, situation slightly dorsally of the bases of pro- and mesothoracic legs; are around articulation of legs each with three minute setae on anterior lobe, and a moderately long seta on posterior lobe. All three pairs of legs well developed, as long as or slightly longer than the height of the thoracic segments in lateral view. *Prothoracic leg.* Coxa bearing 12 minute to short setae and one pore-like sensillum, most in distal coxal half. Trochanter with a very long seta distally on the posterior face, with three moderately long setae and three pores on anterior surface, and two moderately long setae and a group of four pores on posterior surface. Femur with 7 stout moderately long setae and two pores on posterior surface, and three moderately long setae on anterior surface. Tibiotarsus with 10 setae and two pores in the distal third, and two moderately long setae in basal third on anterior surface; posterior surface with a long flat spine-like projection. Pretarsus with a weakly arcuate claw bearing two short but stout setae on anterior surface. Meso- and metathoracic legs slightly longer than prothoracic, but with same morphology and chaetotaxy.

Abdomen (Fig. 6B–C): Abdominal segment I-VII with identical morphology, each with three dorsal lobes; anterior and middle lobe each with 6 short setae dorsally, posterior lobe with 4 short setae; four moderately long setae forming a row between spiracular area and dorsal lobe, spiracular area with one long setae and two minute setae, one anterior and one posterior of the long one; ventral portion of the segment with 5 moderately long setae and one microseta on each side; spiracle minute, the cribrate part largely reduced, with a few evident pores only. Segments VIII-IX larger, with simpler chaetotaxy consisting of a dorsovental rows of moderately long setae, spiracles absent. Raster with four elongate groups of setae, mesal rows with 6–7 short, stout, trichoid setae, lateral rows each with 4 short setae.

Second instar larva (Figs. 4A–D, 5E–G, 5L, 6G–L): Similar in morphology and chaetotaxy to the third instar. Length of the body in uncoiled position (including head): 1.70 mm; maximum width of thorax: 0.37 mm. *Head*: width: 0.43 mm; length: 0.40–0.41 mm, height: 0.22–0.23 mm; head capsule with nearly identical

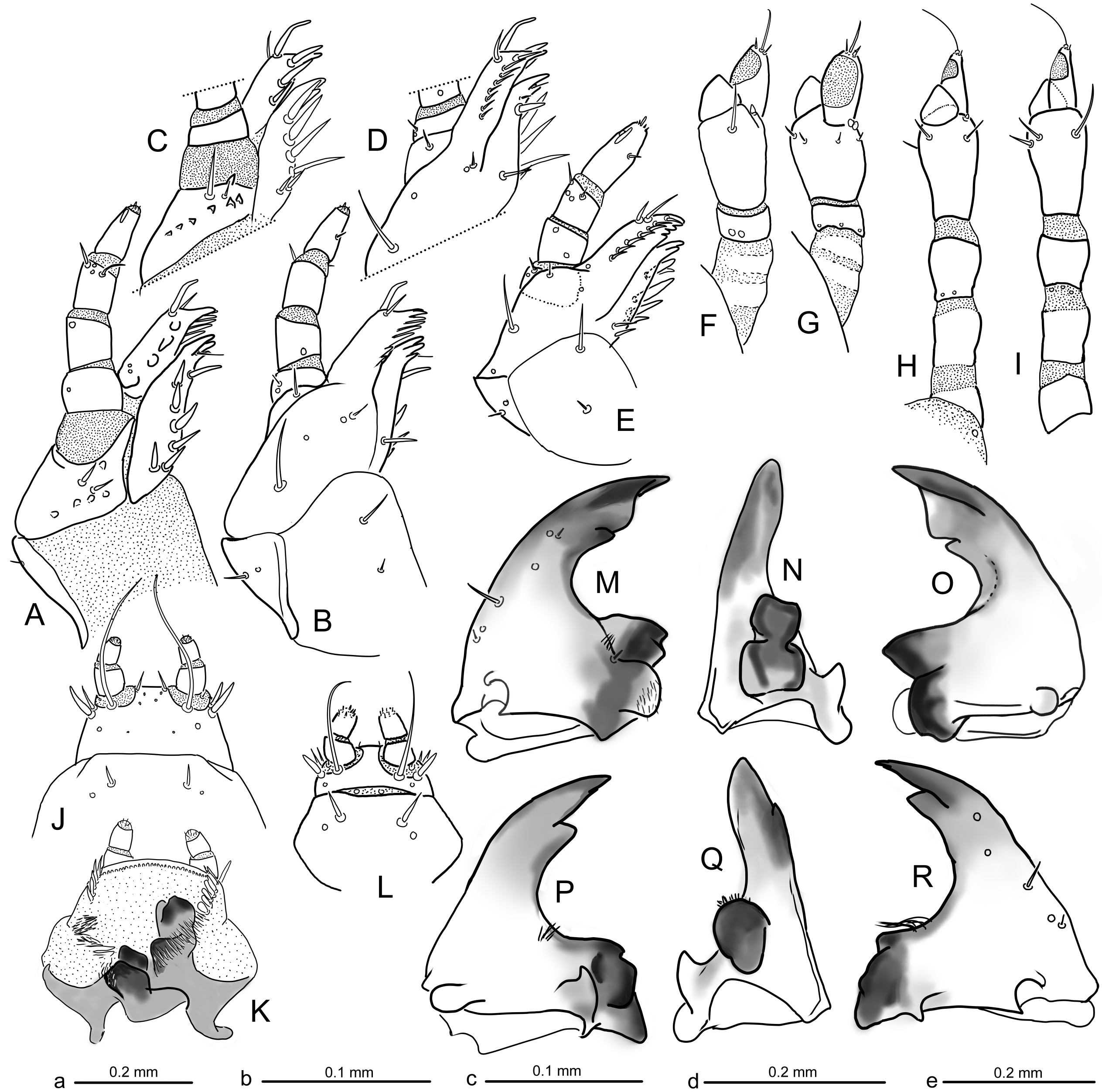

Fig. 5. Head appendages of the larva of *Oxyomus alligator* sp. nov. (E–G, L, second instar, HS3_060L sequenced specimen; A–D, H–K, M–R, third instar, HS03_062L, sequenced specimen). A–E, maxilla: A–B, left maxilla (A, ventral view; B, dorsal view); C–E, right maxilla (C, ventral view; D–E, dorsal view). F–I, antenna (F, H, ventral view; G, I, dorsal view); J–L, labium (J, L, ventral view; K, dorsal view = hypopharynx). M–O, left mandible (dorsal, internal and ventral view); P–R, right mandible (ventral, internal and dorsal view). Scale bars: a for A–D, J–K; b for E, L; c for F–G; d for H–I; e for M–R.

chaetotaxy, just without the short setae present in L3. *Antenna*: relatively shorter and stouter, with the pseudosegments of antennomere 1 more apparent, antennomere 2 very short, antennomere 3 shorter and wider, and antennomere IV slightly club-like; sensorial field on antennomere IV large, covering larger part of dorsal surface and c. one third of surface ventrally. *Maxilla*: with similar morphology and chaetotaxy, only with shortest setae absent, and maxillary palpus with palpomeres I-III short, subequal in length, and palpomere IV the longest. *Labium*: with form, chaetotaxy and proportion of labial palps similar to L3.

Comparison with the larva of *O. sylvestris*: The larva of *O. alligator* sp. nov. is very similar to the larva of the Holarctic *O. sylvestris* (Jerath 1958 1960; Ritcher 1966; Vitner 1996). We only found the following differences: (1) dorsal surface of stipes with 1 + 4–6 denticles (1–2 + 5–6 in *O. sylvestris*) and with two moderately long setae only (with additional minute seta and pore in *O. sylvestris*); (2) epipharynx with protophoba ca. as long as wide, with short and wide cuticular teeth (longer than wide and with narrow and long cuticular teeth in *O. sylvestris*); (3) the molar part of the left mandible only indistinctly subdivided into basal and distal part in dorsal view (with large and more prominent distal part in *O. sylvestris*); (4) the sensilla on

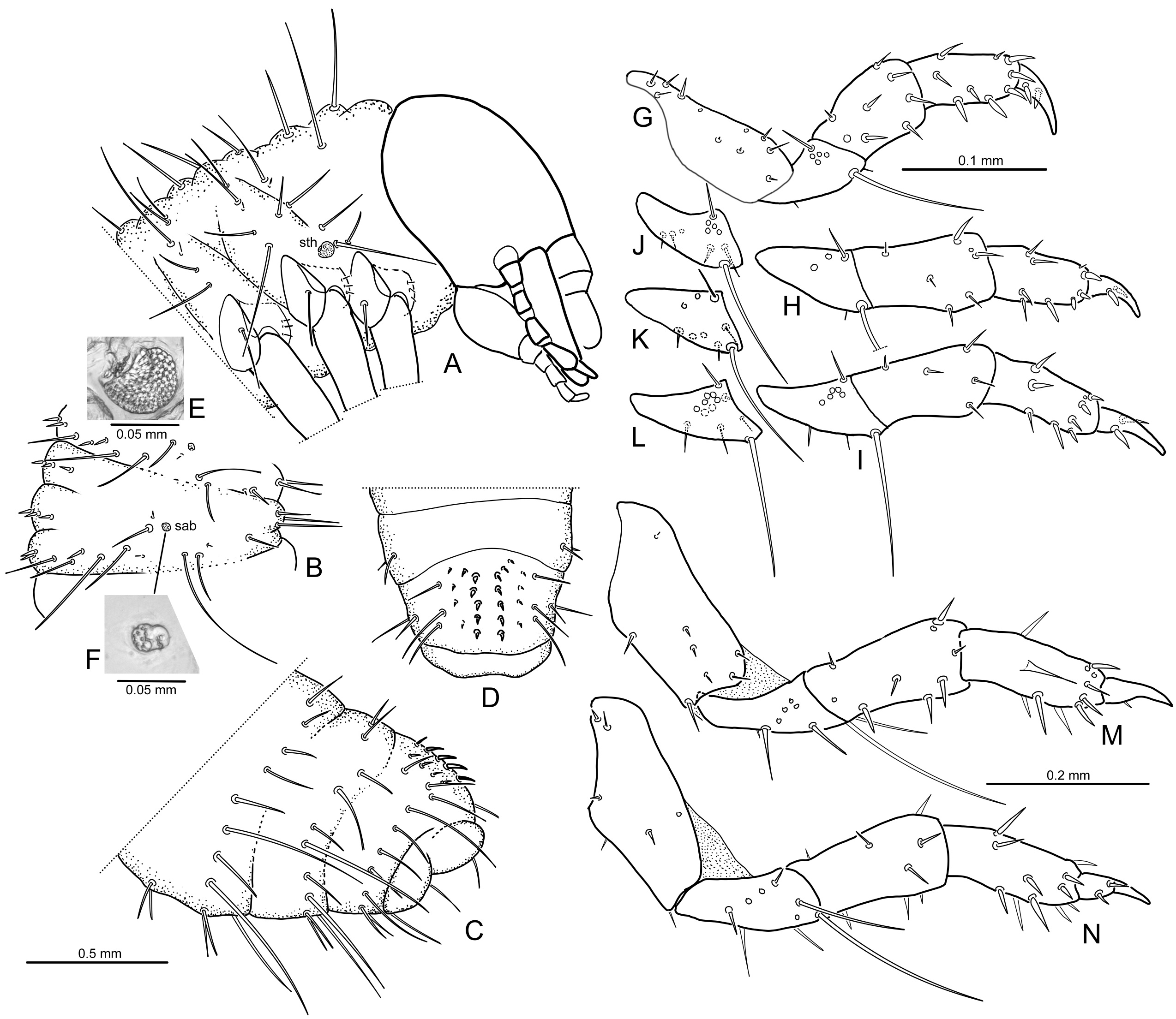

Fig. 6. Thorax and abdomen of the larva of *Oxyomus alligator* sp. nov. (A–F, M–N, third instar, HS3_062L sequenced specimen; G–L, second instar, HS03_060L, sequenced specimen). A, thorax in lateral view; B, abdominal segment III in lateral view; C, abdominal apex in lateral view; D, abdominal apex in ventral view; E, thoracic spiracle; F, abdominal spiracle. G–I, legs of the second instar larva in posterior view (G, prothoracic; H, mesothoracic; I, metathoracic); J–L, trochanters of second instar larva with chaetotaxy of posterior and anterior surfaces (J, prothoracic, K, mesothoracic; L, metathoracic). M–N, prothoracic leg of the third instar larva (M, posterior view; N, anterior view).

palpomere 3 situated at the distal margin (subdistally in *O. sylvestris*); (5) the dorsal setae of tibiotarsus situated more basally than basalmost ventral setae (at the level of basalmost ventral setae in *O. sylvestris*); (6) raster with the mesal row with 6–7 setae, lateral with 4–5 setae (in *O. sylvestris* with 7–8 setae in mesal row and 4–6 setae in lateral row). We also found that the chaetotaxy and surface structures of maxillary stipes, lacinia and galea are asymmetrical in *O. alligator* sp. nov.; this asymmetry is not mentioned in published description of *O. sylvestris* larvae (and those of other Aphodiinae), and we cannot exclude that has been overlooked (and may not be a real difference between the *Oxyomus* species with known larvae).

Collecting circumstances and identification: All examined larvae were collected by sifting leaf litter in a submontane broad-leaf forest with intermixed *Cryptomeria japonica* trees, together with a single adult. *Cox1* of the two larvae (one larger one, one smaller one) were sequenced and found to be conspecific with adults of *Oxyomus alligator* sp. nov. collected at the same locality as well as on other sampled localities in the area. The *cox1* barcodes also confirmed that both instars described above are conspecific.

Oxyomus masumotoi **Nomura, 1973**

(Fig. 7A, 7E, 7J, 7L, 7N)

Material examined: TAIWAN: Hualien County: 1♂, alt. 1050–1250 m, Walami, Zhuoxi, Hualien, TAIWAN, 6–7.VI.2016, F.S. Huang & M. Kiuchi leg.// coll. Masumoto 2017// *Oxyomus masumotoi* (BHHC). Chiayi County: 1♀, Nanshi Logging Road, Yushan Natl. Park, Chiayi, TAIWAN, 23-X-2017, M. Kiuchi leg.// coll. Masumoto 2017// *Oxyomus masumotoi* (BHHC). 1ex, Nanxi logging rd., Alishan Township, alt. 1920m, monkey dung, 22.X.2017, B.H. Ho leg.// BHPC 000-0889 (BHHC). 8 ex, Alishan, Shishan Race, alt. 2320 m, 23.46851°N, 120.85368°E, 16.IX.2021, B.H. Ho & Y. Ho leg. (BHHC). Nantou County: 1ex, Lugu, Mt. Fenghuang observatory, alt. 1770 m, 23°39'39.3"N, 120°48'28.5"E, 14.VII.2021, B.H. Ho leg.// Collected from dung masses of *Muntiacus reevesi micrurus* in the *Cryptomeria japonica* artificial forest. (BHHC). 1ex, Lugu, Mt. Fenghuang, alt. 1800 m, 23°39'15.6"N, 120°48'30.8"E, 12-20.VIII.2021, B.H. Ho & Y. Ho leg., (dung bait PTs) (BHHC). 3exs, Lugu, Mt. Fenghuang, alt. 1800 m, 23°39'15.6"N, 120°48'30.8"E, 19-26. IX.2021, B.H. Ho & Y. Ho leg., (dung bait PTs) (BHHC). 4exs, Xinyi, Shalixian Logging Road, alt. 1600 m, 23.513612°N, 120.911336°E, 12.IV-22.V.2018, I.C. Wang & S.P. Kao leg. (FIT) (CCLI).

Differential diagnosis: *Oxyomus masumotoi* resembles *O. mencli* Minkina, 2016 from Borneo (Sabah: Mt. Kinabalu N.P., Poring Hot Sogs) and *O. nanxiensis* Masumoto, Kiuchi & Wang, 2018 from Taiwan by similar shape of pronotum and elytra. It can be distinguished from *O. mencli* and *O. nanxiensis* as follows: (1) pronotal punctures are large and with long setae; (2) elytra costae shiny, with short micro-setae, elytral intervals dull; (3) elytra relatively shorter, with intermingled rounded punctures on each elytra interval; (4) body strongly convex in lateral view; (5) the 5th elytral costa is short and low, ca. as long as 4th costa and much shorter than 7th costa.

Distribution: *Oxyomus masumotoi* is only known from Taiwan. It is widespread in the mountain areas of central and eastern Taiwan where it occurs in altitudes between 1050–2320 m. It is recorded from the following regions: Nantou County, Chiayi County and Hualien County.

Biology: *Oxyomus masumotoi* inhabits dung masses of muntjac *Muntiacus reevesi*, Formosan serow *Capricornis swinhoei* and macaque *Macaca cyclopis* Swinhoe in mixed primary or secondary *Cryptomeria* forests. It can also be collected in pitfall traps baited with cow dung and/or human dung.

Oxyomus nanxiensis **Masumoto, Kiuchi & Wang, 2018**

(Fig. 7B, 7F, 7H, 7K, 7M, 7O)

Type material examined: Holotype: ♂, Nanxi Logging Road, Yushan Natl. Park, Chiayi, TAIWAN, 23-X-2017, M. Kiuchi leg.// HOLOTYPE *Oxyomus nanxiensis* Masumoto et al., 2018 [printed, red label] (NMNS). Paratypes: 4exs, TAIWAN: Chiayi Co., Nanxi Logging Rd. 11k, alt. 1920 m, Alishan Township, monkey dung, 22.X.2017, B.H. Ho leg.// PARATYPE *Oxyomus nanxiensis* Masumoto et al., 2018 [printed, pink label] (BHHC). 1ex, Nanshi Logging Road 11–12 km, alt. 1850–1950 m, Yushan Natl. Park, Chiayi, TAIWAN// 7.IV.2017, M. Kiuchi, T.-C. Wang & K.-H. Chuang leg.// Coll. Masumoto 2017// PARATYPE *Oxyomus nanxiensis* Masumoto et al., 2018 [printed, pink label]// ex coll. D. Král National Museum Prague, Czech Republic (NMPC).

Material examined: TAIWAN: Chiayi County: 10 ex, Alishan, Shishan Race, alt. 2320 m, 23.46851°N, 120.85368°E, 16.IX.2021, B.H. Ho & Y. Ho leg. (BHHC).

Differential diagnosis: *Oxyomus nanxiensis* resembles *O. masumotoi* Nomura, 1973 from Taiwan by similar body shape. It can be distinguished from *O. masumotoi* as follows: (1) body large, color usually darker; (2) elytra elongate; (3) body weakly convex in lateral view; (4) punctures on the pronotum without long setae; (5) elytral costae shiny, without micro-setae;

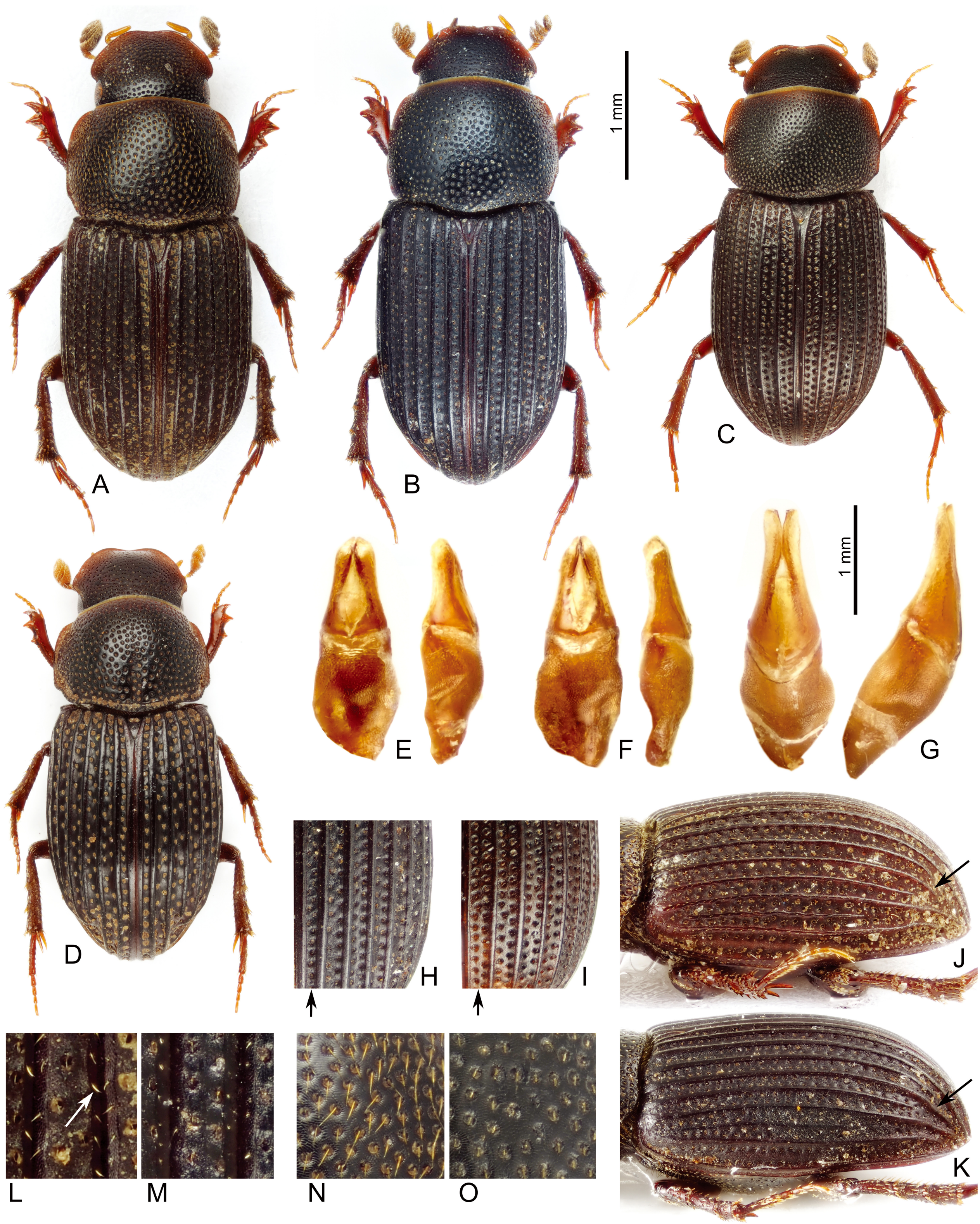

Fig. 7. Taiwanese species of *Oxyomus* and their diagnostic characters. A–D, dorsal habitus (A, *O. masumotoi*; B, *O. nanxiensis*, paratype; C, *O. taipingensis*; D, *O. alligator* sp. nov., paratype). E–G, male genitalia in dorsal and lateral views (E, *O. masumotoi*; F, *O. nanxiensis*; G, *O. taipingensis*). H–I, punctation of the first elytral interval at the level of metathorax (H, *O. nanxiensis*; I, *O. taipingensis*). J–K, elytra in lateral view, showing elytral costae (J, *O. masumotoi*; K, *O. nanxiensis*). L–M, setation of elytral costae (L, *O. masumotoi*; M, *O. nanxiensis*). N–O, punctation of pronotal disc (N, *O. masumotoi*, O, *O. nanxiensis*).

(6) 5th costa long and strongly developed, ca. as long as 7th.

Distribution: *Oxyomus nanxiensis* is only known from Taiwan. It has been collected in mountain areas around Alishan to Yushan National Parks, where it occurs at altitudes between 1850–2320 m. It is recorded from Chiayi County only.

Biology: *Oxyomus nanxiensis* inhabits dung masses of Formosan serow *Capricornis swinhoei* and macaque *Macaca cyclopis*. It occurs sympatrically with *O. masumotoi* in coniferous forest or secondary *Cryptomeria* forests on mountain slopes of Yushan to Alishan areas.

Oxyomus taipingensis Masumoto, Kiuchi & Wang, 2014
(Fig. 7C, 7G, 7I)

Type material examined: Holotype: ♂, Taipingshan, alt. 1950 m, Nanao, Yilan, TAIWAN, 31-III-2014, M. Kiuchi leg.// HOLOTYPE *Oxyomus taipingensis* Masumoto, Kiuchi et Wang, 2014 [printed, red label]// NMNS ENT 7476-6 (NMNS). Paratype: 1ex, Taipingshan, alt. 1950 m, Nanao, Yilan, TAIWAN, 31-III-2014, M. Kiuchi leg.// PARATYPE *Oxyomus taipingensis* Masumoto, Kiuchi et Wang, 2014 [printed, yellow label] (NMNS).

Material examined: TAIWAN: Yilan County: 1ex, Taipingshan, alt. 1950 m, Nanao Township, Yilan County, TAIWAN// 31.III.2014, T.-C. Wang, K.-H. Chuang, M. Kiuchi & K. Masumoto leg.// Coll. Masumoto 2014 (BHHC). Taichung City: 1ex, Heping, Dasyueshan Logging Road 31.5 km, 24°13'37.2"N, 120°58'22.2"E, alt. 2020 m, Formosan serow dung, 1.V.2018, B.H. Ho leg.// *Oxyomus taipingensis* Masumoto, Kiuchi & Wang, 2014 det. B.H. Ho, 2020// BHPC 000-1361 (BHHC). 1ex, Heping, Dasyueshan Logging Road 34 km, 24.240907°N, 120.980256°E, alt. 1940 m, 1.V.2018, B.H. Ho leg.// *Oxyomus taipingensis* Masumoto, Kiuchi & Wang, 2014 det. B.H. Ho, 2018 (BHHC). 1ex, Heping, Chuanxingshan Trail, alt. 1980 m, 24.247688°N, 120.977001°E, 17.IV.2022, B.H. Ho leg. (BHHC). Nantou County: 2exs, Xinyi, Shalixian Logging Road, alt. 1600 m, 23.513612°N, 120.911336°E, 10.III-11.IV.2018, I.C. Wang & S.P. Kao leg. (FIT) (CCLI). 2exs, Xinyi, Shalixian Logging Road, alt. 1600 m, 23.513612°N, 120.911336°E, 12.IV-22.V.2018, I.C. Wang & S.P. Kao leg. (FIT) (CCLI). Kaohsiung City: 1ex, Kaohsiung Hsien, Kuanshan trail above Kaunshanchi Riv., 2550 m, 21.IV.92, A. Smetana [T96]// *Oxyomus taipingensis* Masumoto, Kiuchi & Wang, 2014 David Král det. 2021// ex coll. D. Král

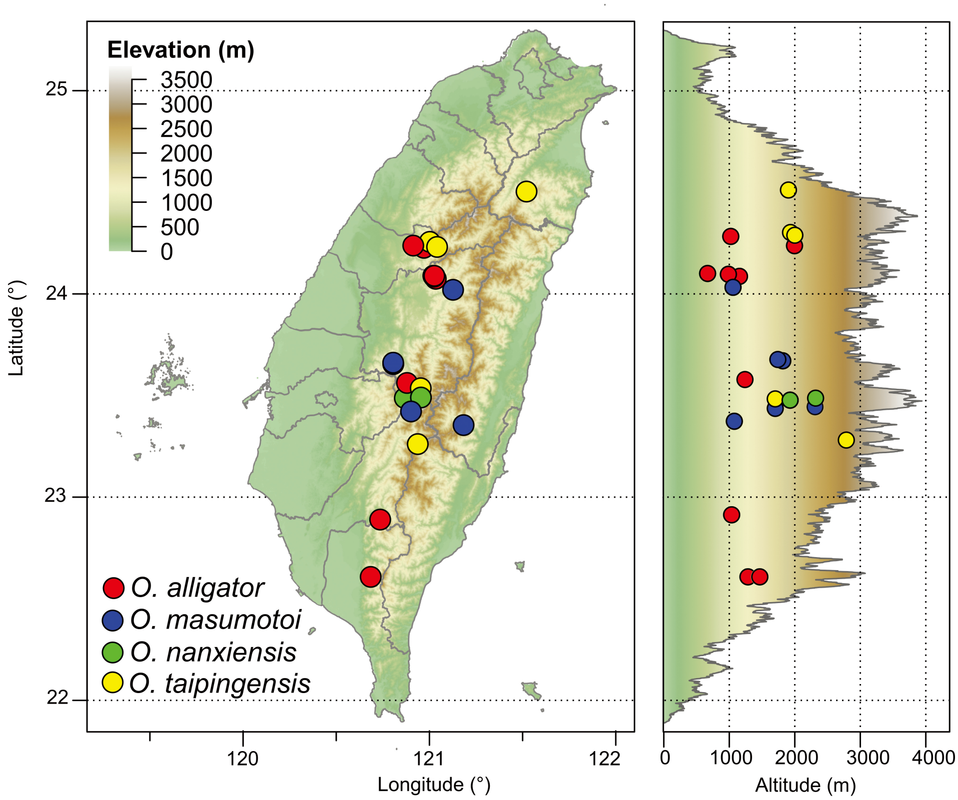

Fig. 8. Distribution of *Oxyomus* species in Taiwan.

National Museum Prague, Czech Republic (NMPC).

Differential diagnosis: *Oxyomus taipingensis* resembles *O. ishidai* Nakane, 1977 from Honshu, Japan (Kanagawa Pref.: Tanzawa Hudakake) by similar shape of elytral punctures and costae. It can be distinguished from *O. ishidai* as follows: (1) pronotum without longitudinal median groove; (2) elytra more strongly convex in lateral view; (3) each elytral interval with two well-separated rows of deep punctures; (4) humeral tooth short. In Taiwan, *O. taipingensis* can be distinguished from other species of the genus by the first elytra interval with two well-separated rows of deep punctures at the level of hind legs.

Distribution: *Oxyomus taipingensis* is only known from Taiwan. It is widespread in the mountain areas of northeastern, central and southern Taiwan where it occurs in altitudes between 1600–2550 m. It has been recorded from the following regions: Yilan County, Taichung City, Nantou County and Kaohsiung City.

Biology: *Oxyomus taipingensis* inhabits dung masses of Formosan serow *Capricornis swinhoei* in coniferous or secondary *Cryptomeria* forests. In some places (*e.g.*, Dasyueshan and Shalixian), it is sympatric with *O. alligator* sp. nov. and/or *O. masumotoi*. Masumoto et al. (2014) recorded this species from dung masses of Formosan sambar *Cervus unicolor swinhoei*.

DISCUSSION

At the moment, Taiwan is the region with the highest known species diversity of *Oxyomus* dung beetles (Schoolmeesters 2022): four endemic species occur in the island, including *O. alligator* sp. nov. described in this study. It stands in contrast to the neighbouring areas: only a single species (*O. ishidai* Nakane, 1977) is known from submontane forests in Japan (Honshu and Shikoku) and no species are known from China and the Philippines. In the Oriental region, four *Oxyomus* species are known from SE Asia (Thailand, Myanmar), four from the Malay Archipelago (Sumatra, Java, Borneo), three from the Himalayas and two from the mountains in southern India (Karnataka, Tamil Nadu). The Taiwanese species are morphologically very disparate: *O. taipingenisis* resembles the Japanese *O.ishidai*, *O. alligator* resembles the SE Asian *O. kocoti*, and the similar and potentially related *O. masumotoi* and *O. nanxiensis* resemble the SE Asian species *O. thailandicus* Masumoto, 1991, *O. kiuchii* Masumoto, 1991, and *O. mencli* Minkina, 2016 from Borneo. The larval morphology of *O. alligator* described here may be only compared with the Holarctic *O. sylvestris* (Jerath 1960; Ritcher 1966; Vitner 1996). Not surprisingly, larvae of both species are very similar, with differences only found in the maxilla and in the abdominal raster. Observed differences in the symmetry of maxillary structures may be, however, a consequence of imprecise previous studies of larvae *O. sylvestris* and need to be confirmed by a re-study of the European species (see larval diagnosis above for details).

The distribution of all four species in Taiwan largely overlap, and two or three species were sometimes collected at the same locality (*e.g.*, *O. masumotoi* and *O. nanxiensis* in Nanxi and Alishan, or *O. alligator* sp. nov., *O. taipingensis* and *O. masumotoi* in Shalixian). Most *Oxyomus* records are from altitudes of 1000–2000 m. *Oxyomus alligator* sp. nov. is the only species recorded from lower altitudes (700 m a.s.l.), and a few records of *O. taipingensis* and *O. nanxiensis* are from areas above 2000 m a.s.l. (the highest record is at 2550 m a.s.l., *O. taipingensis*). *Oxyomus nanxiensis* is the only species which seems locally endemic; it is only known from higher altitudes (1920–2300 m) in Yushan National Park and the Alishan area in Chiayi County. All Taiwanese species have well-developed wings and are occasionally collected in flight intercept traps.

Taiwanese *Oxyomus* species inhabit submontane and montane broadleaf, mixed and conifer forests, including those containing a high proportion of introduced *Cryptomeria japonica*. They can be collected by sifting forest leaf litter, using dung-baited pitfall traps or flight intercept traps, or directly from dung of various forest mammals (macaque *Macaca cyclopis*, muntjac *Muntiacus reevesi*, and Formosan serow *Capricornis swinhoei*). As in most other Aphodiinae, it is expected that the larva develops inside of the dung or dung pellets. Pellets of the muntjac dung were occasionally observed in Huisun Forest Reserve where the larvae of *O. alligator* sp. nov. were collected, and they may have been present among the leaf litter sifted for our samples. The presence of the larvae sifted leaf litter would be possible either when the pellets get broken by a fierce sifting, or may indicate that the larvae may also inhabit the nutrient-rich substrate around the dung. The three localities in Huisun were sampled seven times in 2019–2022, but adults of *Oxyomus alligator* were only found during three visits (May 2019, February 2020 and January 2022) and larvae only once (May 2019). Available records of *Oxyomus* indicate that specimens are collected all around the year in Taiwan, and the absence of *Oxyomus* from many Huisun samples may be a consequence of the absence of mammal dung in the sifted leaf litter.

Most *Oxyomus* species occur in eastern and southeast Asia. They are known from only a few collecting events and seem to be rather locally distributed (*e.g.*, Minkina 2016 2018). Besides that, isolated, locally endemic species are known from

Africa (South Africa, Congo and Angola), Mexico and even Tahiti (Fairmaire 1849; van Lansberge 1886; Dellacasa and Stebnicka 2001; Dellacasa et al. 2014), and a single species (*O. sylvestris*) is widespread across a temperate zone in Eurasia and North America (Ritcher 1966; Schoolmeesters 2022). Interestingly, our limited data show that genetic diversity of *O. alligator* from a single forest reserve is much higher than that of *O. sylvestris* across Europe, indicating a possible difference in population structure and history of tropical versus temperate *Oxyomus* species. The morphology of Taiwanese *Oxyomus* species and their cross island distribution indicates that the Taiwanese fauna is likely of a composite origin, similar to some other leaf litter beetle groups (*e.g.*, Damaška et al. 2021), but molecular data would be desirable to test this assumption.

Acknowledgments: This work and the new species name were registered with ZooBank under urn:lsid:zoobank.org:pub:2ADB1D13-9393-4EAA-9BD8-3A0C880D010E. We thank Hou-Feng Li (National Chung Hsing University, Taiwan), Mei-Ling Chan (National Museum of Natural Science, Taiwan) and Yu-Hsiang Ho (National Chung Hsing University, Taiwan) for lending microscopes to measure adults and take photo of epipharynx, Chun-Lin Li (NTU Experimental Forest, Taiwan), David Král (Charles University, Czech Republic) and Łukasz Minkina (Nowy Targ, Poland) for lending valuable specimens and for consultations, Chi-Ting Hsu (National Chung Hsing University, Taiwan), Wei-Ren Liang (Kyushu University, Japan), Hsing-Che Liu (Hsinchu, Taiwan) and Yun Ho (National Taiwan University, Taiwan) for various assistance during the field survey. This project was supported by the Taiwanese Ministry of Science and Technology project MOST 110-2621-B-110-001. The research activities of MF in the National Museum, Prague, were supported by the Ministry of Culture of the Czech Republic (DKRVO 2019–2023/5.I.c, National Museum, 00023272).

Authors' contributions: BHH co-designed the project, accumulated additional material, identified adult specimens examined prepared the adult systematics part, and participated in drafting the manuscript and its final editing. FSH co-designed the project, collected the Huisun specimens, sequenced the specimens, and participated in drafting the manuscript and its final editing. MF co-designed the project, secured funding, prepared the larval morphology part, and participated in drafting the manuscript and its final editing.

Competing interests: The authors declare that they have no competing interests.

Availability of data and materials: DNA sequences were submitted to the Barcoding of Life Database (sequence IDs: TWOXY001-22 to TWOXY006-22). Original unedited photos and photos taken for comparative purposes, the alignment used to construct the ML tree on figure 1, and the R script used to prepare the distribution map were submitted to Zenodo archive under doi:10.5281/zenodo.7124078. Examined specimens are deposited in collections specified in the manuscript.

Consent for publication: Not applicable.

Ethics approval consent to participate: Not applicable.

REFERENCES

Ahrens D. 2006. The phylogeny of Sericini and their position within the Scarabaeidae based on morphological characters (Coleoptera: Scarabaeidae). Syst Entomol **31:**113–144. doi:10.1111/J.1365-3113.2005.00307.X.

Andújar C, Arribas P, Ruzicka F, Crampton-Platt A, Timmermans MJTN, Vogler AP. 2015. Phylogenetic community ecology of soil biodiversity using mitochondrial metagenomics. Mol Ecol **24:**3603–3617. doi:10.1111/mec.13195.

Arribas P, Andújar C, Salces-Castellano A et al. 2020. The limited spatial scale of dispersal in soil arthropods revealed with whole-community haplotype-level metabarcoding. Mol Ecol **30(1):**48–61. doi:10.1111/mec.15591.

Damaška AF, Konstantinov A, Lee CF, Ruan Y, Mohagan DJ, Fikáček M. 2021. Molecular phylogeny of moss-inhabiting flea beetles from the *Chabria* group (Coleoptera: Chrysomelidae: Alticini) reveals multiple colonizations and radiations in Taiwan. Syst Entomol **46:**915–925. doi:10.1111/SYEN.12502.

Dellacasa G, Dellacasa M, Mann D. 2010. The morphology of the labrum (epipharynx, ikrioma and aboral surface) of adult Aphodiini (Coleoptera: Scarabaeidae: Aphodiinae), and its implications for systematics. Insecta Mundi **132:**1–21.

Dellacasa M, Dellacasa G, Gordon RD. 2014. *Oxyomus mariateresae* new species of Mexican Aphodiini (Coleoptera: Scarabaeidae: Aphodiinae). Insecta mundi **343:**1–3.

Dellacasa M, Stebnicka Z. 2001. A new genus for *Oxyomus morosus* Harold, 1869 (Eupariini) and redefinition of *Oxyomus setosopunctatus* A. Schmidt, 1911 (Aphodiini). Acta Zool Mex (Nueva Ser) **83:**29–34.

Erwin TL. 1982. Tropical forests: their richness in Coleoptera and other arthropod species. Coleopt Bull **36:**74–75.

Fairmaire L. 1849. Essai sur les Coléoptères de la Polynésie. Rev Mag Zool Pure Appliquée **1:**410–422.

Folmer O, Black M, Hoeh W, Lutz R, Vrijenhoek R. 1994. DNA primers for amplification of mitochondrial cytochrome *c* oxidase subunit I from diverse metazoan invertebrates. Mol Mar Biol Biotechnol **3:**294–299.

Grebennikov VV, Scholtz CH. 2004. The basal phylogeny of Scarabaeoidea (Insecta: Coleoptera) inferred from larval morphology. Invertebr Syst **18:**321–348. doi:10.1071/IS03013.

Ho B-H. 2021. A new record species of genus *Odochilus* Harold (Coleoptera: Scarabaeidae: Aphodiinae: Odochilini) from Taiwan. J Trop Coleopterol **2:**13–20. doi:10.53716/jtc.2.2.2.2021.

Huang JP, Lin CP. 2010. Diversification in subtropical mountains: phylogeography, Pleistocene demographic expansion, and evolution of polyphenic mandibles in Taiwanese stag beetle, *Lucanus formosanus*. Mol Phylogenet Evol **57:**1149–1161. doi:10.1016/J.YMPEV.2010.10.012.

Jerath ML. 1958. Systematics of larval Aphodiinae with notes on the biologies of several species (Coleoptera: Scarabaeidae). Unpublished Dissertation, Oregon State College, Corvallis, 161 pp.

Jerath ML. 1960. Notes on larvae of nine genera of Aphodiinae in the United States (Coleoptera: Scarabaeidae). Proc United States Natl Museum **111:**43–94. doi:10.5479/si.00963801.111-3425.43.

Kumar S, Stecher G, Tamura K. 2016. MEGA7: Molecular Evolutionary Genetics Analysis Version 7.0 for Bigger Datasets. Mol Biol Evol **33:**1870–1874. doi:10.1093/MOLBEV/MSW054.

Lawrence JF, Ślipiński A, Seago AE et al. 2011. Phylogeny of the coleoptera based on morphological characters of adults and larvae. Ann Zool **61:**1–217. doi:10.3161/000345411X576725.

Li C, Lu Y, Fang H, Jiang L. 2019. Morphology of the third instar larva of *Colobopterus quadratus* (Coleoptera: Scarabaeidae: Aphodiinae) using scanning electron microscopy. Microsc Res Tech **82:**1372–1379. doi:10.1002/JEMT.23289.

Masumoto K. 1991. Coprophagid-beetles from Northwest Thailand VI. Entomol Rev Japan **46:**27–37.

Masumoto K, Kiuchi M, Wang T-C. 2014. A new species of the genus *Oxyomus* (Coleoptera, Scarabaeidae, Aphodiinae) from the northern part of Taiwan. Elytra, New Ser **4:**267–270.

Masumoto K, Kiuchi M, Wang T-C. 2018. A new species of the genus *Oxyomus* (Coleoptera, Scarabaeidae, Aphodiinae) from the Yushan National Park, Taiwan. Kogane **21:**1–4.

Minkina L. 2018. A new species of the genus *Oxyomus* Dejean, 1833 from Thailand (Coleoptera: Scarabaeidae: Aphodiinae). Stud Reports, Taxon Ser **14:**145–149.

Minkina L. 2016. Three new species of *Oxyomus* Dejean, 1833 (Scarabaeidae: Aphodiini) from the Oriental Region. Stud Report, Taxon Ser **12:**165–176.

Nadkarni NM, Longino JT. 1990. Invertebrates in canopy and ground organic matter in a Neotropical montane forest, Costa Rica. Biotropica **22:**286. doi:10.2307/2388539.

Nakane T. 1977. Eine neue Art der Gattung *Oxyomus* (Coleoptera, Scarabaeidae, Aphodiinae) aus Japan. Bull Natl Museum Nat Sci Ser A **3:**167–168.

Nomura S. 1973. Notes on the coprophagous Lamellicornia from Taiwan. Entomol Rev Japan **25:**37–52.

Ochi T. 2012. Subfamily Scarabaeinae. *In*: Okajima S, Araya K (eds) The standard of scarabaeoid beetles in Japan. Gakken, Japan, pp. 268–307.

Ochi T, Kawahara M, Inagaki M. 2011. Taxonomic notes on some Japanese coprophagous lamellicorn beetles (Coleoptera, Scarabaeoidea) VIII. Descriptions of a new species of the genus Psammodius and a new species of the genus *Trichiorhyssemus* (Aphodiidae) from Tanegashima Is., Southwest Japan. Kogane **12:**69–77.

Paulian R, Scheuern J. 1994. Haroldius Boucomont nouveaux ou peu connus de la région Orientale (Coléoptères Scarabaeidae). Rev suisse Zool **101:**435–440. doi:10.5962/BHL.PART.79913.

Philips TK. 2016. Phylogeny of the Oniticellini and Onthophagini dung beetles (Scarabaeidae, Scarabaeinae) from morphological evidence. Zookeys **2016:**9–57. doi:10.3897/ZOOKEYS.579.6183.

Pittino R, Kawai S. 2007. A new Trichiorhyssemus species from Taiwan, Southwest Japan and Southeast China. Kogane **8:**67–74.

Ritcher P. 1966. White grubs and their allies. A study of North American Scarabaeoid larvae. Oregon State University Press, Corvallis, 219 pp.

Schoolmeesters P. 2022. World Scarabaeidae Database. *In*: Bánki O, Roskov Y, Döring M, et al. (eds) Catalogue of Life Checklist (Version 2022-04-11). doi:10.48580/dfpk-38g.

Šípek P, Gill BD, Grebennnikov VV. 2009. Afromontane Coelocorynus (Coleoptera: Scarabaeidae: Cetoniinae): Larval descriptions, biological notes and phylogenetic placement. **106:**95–106. doi:10.14411/EJE.2009.014.

Stebnicka ZT. 2013. A revision of the Indonesian species of *Saprosites* Redtenbacher, 1858 (Coleoptera: Scarabaeidae: Aphodiinae: Eupariini). Acta Zool Cracoviensia **55:**13–45. doi:10.3409/AZC.55_2.13.

Stork NE, Grimbacher PS. 2006. Beetle assemblages from an Australian tropical rainforest show that the canopy and the ground strata contribute equally to biodiversity. Proc R Soc B Biol Sci **273:**1969–1975. doi:10.1098/rspb.2006.3521.

Tsai C-L, Yeh W-B. 2016. Subspecific differentiation events of montane stag beetles (Coleoptera, Lucanidae) endemic to Formosa island. PLoS ONE **11:**e0156600. doi:10.1371/journal.pone.0156600.

van Lansberge JW. 1886. Scarabaeides, buprestides et cerambycides de l'Afrique occidentale, envoyes au Musee de Leyde par MM. Veth et Van der Kellen (Note XIII). Notes from Leyden Museum **8:**69–120.

Verdu JR, Galante E. 2000. Larval morphology and biology of two species of *Aphodius* (*Plagiogonus*) from the Iberian Peninsula (Coleoptera: Scarabaeidae: Aphodiinae). Eur J Entomol **97:**395–401. doi:10.14411/eje.2000.060.

Vitner J. 1996. Larvy středoevropských druhů podčeledi Aphodiinae (Coleoptera: Scarabaeidae) [Larvae of central European species of the subfamily Aphodiinae (Coleoptera: Scarabaeidae)]. Unpublished Ph.D. dissertation, Department of Zoology, Charles University, Prague, 269 pp + 1686 figs.